

# Sparse approximate solution of fitting surface to scattered points by MLASSO model

Yong-Xia Hao<sup>1</sup>, Chong-Jun Li<sup>2,\*</sup> & Ren-Hong Wang<sup>2</sup>

<sup>1</sup>*Faculty of Science, Jiangsu University, Zhenjiang 212000, China;*

<sup>2</sup>*School of Mathematical Sciences, Dalian University of Technology, Dalian 116024, China;*

*Email: yongxiahaoujs@ujs.edu.cn; chongjun@dlut.edu.cn; renhong@dlut.edu.cn*

Received ; accepted

**Abstract** The goal of this paper is to achieve a computational model and corresponding efficient algorithm for obtaining a sparse representation of the fitting surface to the given scattered data. The basic idea of the model is to utilize the principal shift invariant (PSI) space and the  $l_1$  norm minimization. In order to obtain different sparsity of the approximation solution, the problem is represented as a multilevel LASSO (MLASSO) model with different regularization parameters. The MLASSO model can be solved efficiently by the alternating direction method of multipliers. Numerical experiments indicate that compared to the AGLASSO model and the basic MBA algorithm in [35], the MLASSO model can provide an acceptable compromise between the minimization of the data mismatch term and the sparsity of the solution. Moreover, the solution by the MLASSO model can reflect the regions of the underlying surface where high gradients occur.

**Keywords** Sparse solution, Principle shift invariant space,  $L_1$  norm minimization, Alternating direction method of multipliers, MLASSO model

**MSC(2010)** 65D17, 65K99

**Citation:** Y-X Hao, C-J Li, R-H Wang. SCIENCE CHINA Mathematics journal sample. Sci China Math, 2013, 56, doi: 10.1007/s11425-000-0000-0

## 1 Introduction

Sparse representation of a function via a linear combination of a small number of functions has recently received a lot of attention in several mathematical fields such as approximation theory [13, 33, 41, 42], compressed sensing, signal and image processing [7–10] etc. The problem can be described as follows. Consider a linearly dependent set of  $n$  functions  $\{\varphi_i\}_{i=1}^n$  and a function  $f$  represented as  $f = \sum_{i=1}^n X_i \varphi_i$ . Since the set of functions is not linearly independent, this representation is not unique. The problem is then to find the sparsest solution, i.e., the coefficient vector  $X = (X_1, X_2, \dots, X_n)$  has as many zero components as possible (referred to minimizing the  $l_0$  norm of the vector  $X$ ). This optimization problem is NP-hard, since the  $l_0$  norm is nonconvex and discontinuous. Hence, much attention has been paid to solutions minimizing  $\|X\|_1 = \sum_{i=1}^n |X_i|$  instead.

In this paper, we consider the problem of reconstructing a surface from scattered data using a sparse representation. The scattered data fitting problem arises in many applications, such as signal processing, computer graphics and neural networks [32]. In a typical scattered data reconstruction problem, we are given a set of scattered points  $\Xi = \{x_1, x_2, \dots, x_N\} \subseteq \mathbb{R}^2$  and associated noisy function values

\*Corresponding author

$\tilde{f} = f|_{\Xi} + \mathbf{n} = \{f_1, f_2, \dots, f_N\}$ , where  $\mathbf{n}$  is the error vector. Then we seek a function  $g$  which fits the given data  $\{(x_i, f_i)\}_{i=1}^N$  well. There are a lot of existing methods and algorithms in the literature. Various methods can be found in a survey on scattered data interpolation [38]. For approximation methods, B-splines have a solid mathematical foundation and have been used in many literatures, such as [34, 51] etc. Wavelet frames have also been used to reconstruct implicit surfaces from unorganized point sets in  $\mathbf{R}^3$  [16]. In order to control the local and global fitting error simultaneously, adaptive methods are presented in [11, 44]. The adaptivity is achieved by a portion of the data with a patch, testing the fit for satisfaction within a given tolerance, and subdividing the patch if the tolerance is not met [23]. In addition, several approximation methods employ a multilevel structure to approximate data efficiently. In particular, a multilevel scheme based on B-splines is proposed in [35] to approximate scattered data. These methods run on the approximation space  $S = \bigcup_{j=1}^J S_j$ , where  $S_j \subseteq S_{j+1}$  are principal shift invariant (PSI) spaces generated by a single compactly supported function  $\varphi$ . The multilevel approximation procedure is as follows: for each level  $j$ , the point set  $(\Xi, \Delta g_{j-1})$  is approximated by a function  $g_j \in S_j$  obtained by the least square method, where  $\Delta g_{j-1}|_{\Xi} = \tilde{f} - (g_1 + \dots + g_{j-1})|_{\Xi}$ . The procedure is terminated until certain conditions are satisfied. Then the final approximation surface is

$$g = g_1 + g_2 + \dots + g_J, \quad g_j \in S_j, \quad j = 1, \dots, J.$$

However, the methods above do not produce the sparse representation of the surface.

In this paper, we present an efficient method to obtain a sparse representation of the fitting surface to the given scattered points. We still choose the space  $S$  defined above as the approximation space. But instead of using the multilevel scheme, we put all the basis functions of  $S_j, 1 \leq j \leq J$  together as a frame of  $S$ . Denote the basis functions of  $S_j$  as  $\{\varphi_i^j\}_{i=1}^{n_j}, 1 \leq j \leq J$ , then  $S = \text{span}\{\varphi_i^j\}_{i,j=1}^{n_j, J}$ . We then try to find the fitting surface  $g \in S$  as:

$$g = \sum_{j=1}^J g_j, \quad g_j = \sum_{i=1}^{n_j} X_i^j \varphi_i^j.$$

Since the functions  $\{\varphi_i^j\}_{i,j=1}^{n_j, J}$  are linearly dependent, the representation of  $g$  as above is not unique and we will seek a relatively sparse one. The choice of the space  $S$  makes a sparse representation of  $g$  exist and the function  $\varphi_i^j$  can be constructed in a multilevel way. We use the similar approach as those used in compressed sensing, i.e., to use the  $l_1$  norm of the coefficient vector as the regularization term. Thus, the problem can be represented by the following minimization

$$\min_{g \in S} \sum_{i=1}^N (g(x_i) - f_i)^2 + \sum_{j=1}^J \lambda_j \|\mathbf{X}_j\|_1, \quad (1.1)$$

where  $\mathbf{X}_j = (X_1^j, \dots, X_{n_j}^j), 1 \leq j \leq J$  are coefficient vectors. The parameters  $\lambda_j > 0, j = 1, \dots, J$  are called the regularization parameters, which serve as a weight to adjust the balance between the two terms. Large values of  $\lambda_j$  will lead to a sparse function  $g$ , at the cost of a potentially large fitting error, while small values of  $\lambda_j$  will lead to a small fitting error, but with a potentially not too sparse fitting function  $g$ . In addition, different values of  $\lambda_j$  can lead to different sparsity of  $g$ . Let  $\mathbf{f}$  denote the column vector  $\{f_i\}_{i=1}^N$ , then the formulation (1.1) is equivalent to the following minimization:

$$\min_{\mathbf{X}_j, 1 \leq j \leq J} \left\| \sum_{j=1}^J \mathbf{A}_j \mathbf{X}_j - \mathbf{f} \right\|_2^2 + \sum_{j=1}^J \lambda_j \|\mathbf{X}_j\|_1, \quad (1.2)$$

where  $\mathbf{A}_j$  is the observation matrix defined by

$$\mathbf{A}_j(i, k) = \varphi_k^j(x_i), \quad i = 1, 2, \dots, N, \quad k = 1, 2, \dots, n_j, \quad j = 1, 2, \dots, J.$$

For the case  $\lambda_1 = \dots = \lambda_J$ , the model reduces to the model presented in [30]. Moreover, the  $l_1$  related minimization resulting from our proposed model can be efficiently solved using the alternating direction method of multipliers (ADMM) [24, 54].

This framework combines the ideas developed in compressed sensing with well-known concepts arising in adaptive and multilevel finite element methods. The solution of the  $l_1$  minimization problem and the multilevel basis functions are used to control the grid refinement and adaptivity. Since we aim at finding a sparse representation of the surface, we discard those coefficients which are smaller than a certain threshold. Then only large coefficients of the solution are left which indicate important contributions of the underlying surface. Moreover, these large coefficients belong to the parts of the surface that have large fluctuations. It seems a little similar for our method and the approach in [15], both using the PSI space. However, the method in [15] was used to approximate functions expressed as a infinite sum of wavelet decomposition by a finite sum, while we deal with scattered data fitting problem by representing the fitting function as a finite sum directly with certain accuracy and more sparse coefficients. The behavior of our method is demonstrated via four examples: a discontinuous function, a non-smooth function, a smooth function and the Franke test function. In addition, we compare the numerical results with the AGLASSO model and the basic MBA algorithm in [35] followed by the same thresholding.

The rest of the paper is organized as follows. In the next section, we recall the main ingredients of the PSI space which will be used here. Moreover, we will propose the sparsity based regularization model for scattered data fitting. In Section 3, the ADMM algorithm will be applied to solve the minimization problem resulted from the proposed model. Numerical experiments are also performed to illustrate the algorithm. Section 4 is the conclusion.

## 2 Sparse solution of PSI approach to scattered data approximation

For a given set of scattered points  $\{x_i\}_{i=1}^N \subseteq \Omega \subseteq \mathbb{R}^2$  and the corresponding noisy data  $\{f_i\}_{i=1}^N$ , our task is to reconstruct a fitting surface with a sparse representation.

### 2.1 PSI space and $l_1$ regularization

Let  $\Omega \subseteq \mathbb{R}^2$  be a bounded domain of interest where all data lie in and let  $\varphi$  be a carefully chosen, compactly supported function (e.g. uniform B-spline, box spline, radial basis functions). Denote

$$\Lambda = \{k \in \mathbb{Z}^2 : \text{supp}(\varphi(\cdot/h - k)) \cap \Omega \neq \emptyset\}, \quad S^h(\varphi, \Omega) = \{f | f = \sum_{k \in \Lambda} c_k \varphi(\cdot/h - k)\},$$

where  $h > 0$  is a scaling parameter that controls the refinement of the space. Denote  $S_j = S^{h/2^{j-1}}(\varphi, \Omega)$ ,  $S_1 \subseteq \dots \subseteq S_J$ , we then look for a function  $g \in S_J$  which fits closely the given data. Then  $g$  is composed of a sequence of functions as

$$g = g_1 + g_2 + \dots + g_J,$$

where  $g_i \in S_i$ ,  $i = 1, 2, \dots, J$ .

Here we choose a proper PSI space generated by B-spline as the approximation space  $S$  since it enjoys desirable properties for data fitting. It has a simple structure and provides good approximation to smooth functions, which leads to simple and accurate algorithms. Moreover, it can be associated to a wavelet or frame system and hence one can solve the fitting problem by making use of the advantages that a wavelet (frame) system can offer [30]. These advantages include sparse approximation of functions in the wavelet (frame) domain, multilevel structure of basis functions, adaptivity to the data, norm equivalence, etc.

Recall that a function  $\varphi$  is said to satisfy the Strang-Fix conditions of order  $m$  if

$$\hat{\varphi}(0) \neq 0, \quad D^\alpha \hat{\varphi}(2\pi j) = 0, \quad \forall j \in \mathbb{Z}^2 \setminus 0, \quad |\alpha| < m.$$

Denote

$$W_2^m = \{f \in L_2(\mathbb{R}^2) : \|f\|_{W_2^m} = \sqrt{2\pi} \|(1 + |\cdot|^m) \hat{f}\|_{L_2(\mathbb{R}^2)} < +\infty\},$$

where  $\hat{f}$  is the Fourier transform of the function  $f$  and  $|\cdot| = \|\cdot\|_2$  denotes the Euclidean norm. Then if  $\varphi$  satisfies the Strang-Fix conditions [14, 31], a PSI space provides good approximation to  $W_2^m$  (see [14, 31]),

i.e.,  $\varphi$  satisfies the Strang-Fix conditions of order  $m$  if and only if for all  $f \in W_2^m$ ,

$$\inf_{s \in S^h(\varphi, \Omega)} \|f - s\|_{L^2(\mathbb{R}^2)} = O(h^m).$$

Particularly, the B-spline  $B_m$  of order  $m$  satisfies the Strang-Fix conditions of order 2 for all  $m \geq 2$  [16]. For more detailed discussions on PSI space, see [14].

Obviously, the union set of the basis functions of  $S_j$  is not linearly independent. Thus the representation of  $g$  is not unique and we want to determine a relatively sparse one, i.e., a representation with as many vanishing coefficients as possible. Every function  $g_j \in S_j$  can be written as

$$g_j = \sum_{k \in I_j} X_k^j \varphi(2^{j-1}x/h - k),$$

where

$$I_j = \{k \in \mathbb{Z}^2, \text{supp}(\varphi(2^{j-1} \cdot /h - k)) \cap \Omega \neq \emptyset\}.$$

Let  $\mathbf{X}_j$  and  $\mathbf{f}$  denote the column vector  $\{X_k^j\}_{k \in I_j}$  and  $\{f_i\}_{1 \leq i \leq N}$  respectively, then the problem can be formulated as follows.

$$\min_{\mathbf{X}_j, 1 \leq j \leq J} \left\| \sum_{j=1}^J A_j \mathbf{X}_j - \mathbf{f} \right\|_2^2 + \sum_{j=1}^J \lambda_j \|\mathbf{X}_j\|_1, \quad (2.1)$$

where  $A_j$  is the observation matrix defined by

$$A_j(i, k) = \varphi(2^{j-1}x_i/h - k), \quad k \in I_j, \quad i = 1, 2, \dots, N, \quad j = 1, 2, \dots, J.$$

Obviously, the model (2.1) balances the fitting accuracy and the  $l_1$  norm. In order to achieve a sparse representation, small coefficients are neglected. That is, after obtaining the solution  $\{\mathbf{X}_j\}_{j=1}^J$  of the model (2.1), we discard the small elements of  $\mathbf{X}_j, 1 \leq j \leq J$ . Then the final solution only has large values left which indicate important contributions (fluctuations) of the real surface. Furthermore, comparing with the multilevel approximation approach given in [35], our method has the advantages of simplicity. Another important distinction is that it can be interpretable as a sparse strategy for reconstructing scattered data.

## 2.2 The MLASSO model

The model (2.1) is related to the LASSO model in some extent. Recall that the mathematical model of LASSO is:

$$\min_{\mathbf{X}} \|\mathbf{A}\mathbf{X} - \mathbf{f}\|_2^2 + \mu \|\mathbf{X}\|_1.$$

It was proposed originally in [48], and plays a very influential role in variable selection and dimensionality reduction. The Group LASSO (GLASSO) model proposed in [53] solves the convex optimization problem:

$$\min_{\mathbf{X}_j, 1 \leq j \leq J} \left\| \sum_{j=1}^J A_j \mathbf{X}_j - \mathbf{f} \right\|_2^2 + \mu \sum_{j=1}^J \|\mathbf{X}_j\|_2,$$

where  $\mu > 0$  is a regularization parameter. The GLASSO model was proposed to perform variable selection on groups of variables for linear regression models. It has many applications in areas such as computer vision, data mining, etc. Meier et al. in [39] extended the GLASSO to logistic regression. The GLASSO does not, however, yield sparsity within a group. Moreover, GLASSO suffers from estimation inefficiency and selection inconsistency. To remedy these problems, the adaptive GLASSO method (AGLASSO) is proposed in [49] as:

$$\min_{\mathbf{X}_j, 1 \leq j \leq J} \left\| \sum_{j=1}^J A_j \mathbf{X}_j - \mathbf{f} \right\|_2^2 + \sum_{j=1}^J \mu_j \|\mathbf{X}_j\|_2.$$

Obviously, the model (2.1) reduces to the LASSO model when  $\mu = \lambda_1 = \cdots = \lambda_J$ . Moreover, the model (2.1) acts like the LASSO at the multilevel. Therefore, we denote the model (2.1) as the multilevel LASSO model (MLASSO). Compared with the AGLASSO model, the MLASSO model considers an additional penalty on the  $l_1$  norm instead of  $l_2$  norm of the regression coefficient vector, and it produces as election of variables with sparsity among different levels. It is known that when  $l_2$  norm regularization term is applied to the data set, the resulting surface tends to be smooth without sharp discontinuities but have undesirable oscillations near the discontinuities [30]. Recently, several surface reconstruction approaches have been proposed to preserve surface discontinuity by replacing  $l_2$  regularization using more sophisticated regularization, e.g., the Huber approximation of  $l_2$  norm of function derivatives in [47], the local kernel regularization in [25] and the non-local means regularization in [16]. In our method, we use the  $l_1$  regularization instead, in order to obtain the relatively sparse solution. The regularization term  $\|\cdot\|_1$  in (2.1) penalizes the roughness of the solution.

### 2.3 The parameter selection

The determination of the proper value of  $\{\lambda_j\}$  in the MLASSO model is an important problem and depends on the variance of the noise  $\mathbf{n}$ , the properties of  $\{A_j\}$  and  $\|\cdot\|_1$ . An appropriate choice of the regularization parameters is of vital importance for the quality of the resulting estimate and has been the subject of extensive research [3].

In recent years, there has been a growing interest in sophisticated regularization techniques which use multiple constraints as a mean of improving the quality of the solution [3]. Among them, only a few papers discussed the choice of multiple regularization parameters. However, most of them discuss the case that the regularization term is the  $l_2$  norm. For example, a multi-parameter generalization of heuristic L-curve has been proposed in [3], a knowledge of noise (covariance) structure is required for a choice of parameter in [1, 2, 12], some reduction to a single parameter choice is suggested in [6]. At the same time, the discrepancy principle, which is widely used and known as the first parameter choice strategy proposed in the regularization theory [40], has been discussed in a multi-parameter context in [37]. Of course, there might be many different methods to choose the regularization parameters satisfying certain principle. In fact, the choice of the regularization parameters in the regularization modes, such as the LASSO model and the standard Tikhonov regularization model, have not yet solved. No choice is available for all the models. Basically, different models need different methods to decide the parameters, and even the same one may have different methods to choose, such as [27, 28, 49, 50, 55].

For the MLASSO model, instead of discussing similar methods as listed above, we propose two simple criteria for the choice of the parameters  $\{\lambda_j\}_{j=1}^J$  according to the sparsity and the support of the basis functions of the different levels. On one hand, since the length of  $\mathbf{X}_j$  is less than that of  $\mathbf{X}_{j+1}$ , so if one wants to obtain sparser solution, the parameters of the last several levels should be larger. In particular, choosing the same value for all the parameters, i.e.,  $\lambda_1 = \cdots = \lambda_J$ , obtains the global sparsity in the whole space  $S$ . On the other hand, the support of the basis functions of the  $j$ -th level is larger than that of the  $(j+1)$ -th level, so if one wants smaller support, the parameters of the first several levels should be larger. Hence, the more appropriate choice of the parameters is to make the parameters of the first and last several levels greater than the middle several levels. We can only give such a qualitative guideline, since quantitative guidance for regularization parameters is rarely available. In this way, the solution has smaller support and sparser representation with good approximation accuracy. Numerical results also confirm this selection method as shown in the Tables 1-8. Moreover, in contrast with the methods listed above, this choice is easier and cheaper in the sense of computational cost.

Based on the above, the proposed method offers some interesting advantages:

- 1) Related with the LASSO model, the MLASSO model has a strong statistical background;
- 2) Compared to the LASSO model, the parameters in the MLASSO model can be chosen differently, thus one can attain high flexibility for the approximation accuracy and the sparsity of the solution;
- 3) Compared to the AGLASSO model, the MLASSO model can provide the sparsity of the solution by choosing different parameters and the distribution of the solution can reflect the large fluctuations of the

underlying surface;

4) Utilizing the ADMM algorithm, the MLASSO model can be efficiently solved.

### 3 Numerical algorithm

#### 3.1 Algorithm

In this section, we use the ADMM algorithm to solve the minimization model (2.1) for experimental evaluation. It turns out that ADMM is equivalent to or closely related to many famous algorithms, such as the Douglas-Rachford splitting method in PDE literature [18, 19, 36], the Bregman iterative algorithms for  $l_1$  problems in signal processing [26] and many others. In particular, we refer to [21, 45, 46, 52] for the relationship between ADMM and the split Bregman iteration scheme which is very influential in the area of image processing. Convergence analysis of the ADMM was given in [5, 20, 29].

In order to solve the MLASSO model (2.1) and guarantee the convergence, we denote

$$A = (A_1, A_2, \dots, A_J), \quad \mathbf{X} = (\mathbf{X}_1^T, \mathbf{X}_2^T, \dots, \mathbf{X}_J^T)^T,$$

$\lambda = \text{diag}(\lambda_1, \lambda_2, \dots, \lambda_J)$  is a diagonal matrix with  $\lambda_j, j = 1, \dots, J$  as the main diagonal. Then we can rewrite (2.1) as

$$\min_{\mathbf{X}} \|\mathbf{A}\mathbf{X} - \mathbf{f}\|_2^2 + \|\lambda\mathbf{X}\|_1. \quad (3.1)$$

By introducing an auxiliary variable  $\mathbf{d} = \lambda\mathbf{X}$ , we convert the unconstrained minimization problem (3.1) into a constrained one:

$$\min_{\mathbf{X}, \mathbf{d}=\lambda\mathbf{X}} \|\mathbf{A}\mathbf{X} - \mathbf{f}\|_2^2 + \|\mathbf{d}\|_1. \quad (3.2)$$

In this way, the MLASSO model (2.1) is turned into a classical  $l_1$  minimization problem. The augmented Lagrangian function of problem (3.2) is

$$L(\mathbf{X}, \mathbf{d}, \mathbf{b}) = \|\mathbf{A}\mathbf{X} - \mathbf{f}\|_2^2 + \|\mathbf{d}\|_1 + \frac{\beta}{2} \|\lambda\mathbf{X} - \mathbf{d}\|_2^2 + \langle \mathbf{b}, \lambda\mathbf{X} - \mathbf{d} \rangle,$$

where  $\beta > 0$  is a parameter of the algorithm. Then by applying the ADMM method, given the initialization  $\{\mathbf{X}^0, \mathbf{d}^0, \mathbf{b}^0\}$  and the parameters  $\{\lambda_j\}_{j=1}^J$ , it results in the following optimization algorithm:

$$\begin{cases} \mathbf{X}^{k+1} = \arg \min_{\mathbf{X}} \|\mathbf{A}\mathbf{X} - \mathbf{f}\|_2^2 + \frac{\beta}{2} \|\lambda\mathbf{X} - \mathbf{d}^k + \frac{\mathbf{b}^k}{\beta}\|_2^2, \\ \mathbf{d}^{k+1} = \arg \min_{\mathbf{d}} \|\mathbf{d}\|_1 + \frac{\beta}{2} \|\lambda\mathbf{X}^{k+1} - \mathbf{d} + \frac{\mathbf{b}^k}{\beta}\|_2^2, \\ \mathbf{b}^{k+1} = \mathbf{b}^k + (\lambda\mathbf{X}^{k+1} - \mathbf{d}^{k+1}). \end{cases} \quad (3.3)$$

First of all, the above algorithm is convergent, since it is just the classical ADMM for two block of variables. Secondly, the system can be simply solved. The first step of each iteration in (3.3) is

$$(2A^T A + \beta\lambda^T \lambda)\mathbf{X} = 2A^T \mathbf{f} + \beta\lambda^T (\mathbf{d}^k - \frac{\mathbf{b}^k}{\beta}).$$

This linear system is positive definite and therefore it can be solved by the conjugate gradient method (CG). When the matrix is ill-posed, i.e., its condition number is huge, the convergence rate of the CG will be very slow. Under this case, the preconditioned CG [4, 22, 43] can be used instead to reduce the condition number of the coefficient matrix and improve the convergence speed. The second subproblem has a simple analytical solution based on soft-thresholding operator [17], that is

$$\mathbf{d}^{k+1} = T_{\frac{1}{\beta}}(\lambda\mathbf{X}^{k+1} + \frac{\mathbf{b}^k}{\beta}),$$

where  $T_\theta$  is the soft-thresholding operator defined by

$$T_\theta : x = [x_1, x_2, \dots, x_M] \rightarrow T_\theta(x) = [t_\theta(x_1), t_\theta(x_2), \dots, t_\theta(x_M)],$$

where

$$t_\theta(\xi) = \text{sgn}(\xi) \max\{0, |\xi| - \theta\}.$$

The complete description of the algorithm for solving the model (2.1) is provided as Algorithm 1 as follows:

**Algorithm 1.** (Adapted ADMM for solving the MLASSO model (2.1))

Step 1) Set  $J$  and the initial values  $\{\mathbf{X}^0, \mathbf{d}^0, \mathbf{b}^0\}$ , choose appropriate sets of parameters  $\{\lambda_j\}_{j=1}^J$ ,  $\beta$  and two thresholds  $\sigma, \epsilon$ ;

Step 2) For  $k = 0, 1, \dots$ , perform the iteration (3.3) until convergence;

Step 3) Assume  $\tilde{\mathbf{X}}$  is the solution obtained from Step 2), if  $|\tilde{\mathbf{X}}(i)| \leq \sigma$ , i.e., the absolute value of the  $i$ -th element of  $\tilde{\mathbf{X}}$  is less than  $\sigma$ , set  $\tilde{\mathbf{X}}(i) = 0$ ;

Step 4) The final solution  $\mathbf{X}$  are  $\tilde{\mathbf{X}}$  after the treatment of Step 3).

In our numerical experiments, the initializations are  $\mathbf{X}^0 = \mathbf{d}^0 = \mathbf{b}^0 = 0$ ,  $\beta = 1$  and the stopping criteria is

$$\|\mathbf{d}^k - \lambda \mathbf{X}^k\|_2 \leq \epsilon.$$

### 3.2 Numerical experiments

Given a test function  $f(x, y)$  with  $\Omega = [-1, 1] \times [-1, 1]$ , we first sample data points with certain noises from it, i.e.,  $\{(x_i, y_i, f(x_i, y_i) + \varepsilon_i)\}$ . The error vector  $\mathbf{n} = (\varepsilon_i)_i$ , whose entries consist of the pseudorandom values drawn from the standard uniform distribution on the open interval  $(-\max_i \frac{|f(x_i, y_i)|}{10}, \max_i \frac{|f(x_i, y_i)|}{10})$ . Then apply different methods to obtain the approximation function  $g$ . The difference between  $f$  and  $g$  is measured by computing the normalized RMS (root mean square) error [35]. That is,

$$RMS = \sqrt{\frac{\sum_{i,j=1}^{M_1, N_1} (g(\tilde{x}_i, \tilde{y}_j) - f(\tilde{x}_i, \tilde{y}_j))^2}{M_1 N_1}},$$

where  $\tilde{x}_i = -1 + \frac{2i}{M_1-1}$ ,  $i = 0, 1, \dots, M_1 - 1$ ,  $\tilde{y}_j = -1 + \frac{2j}{N_1-1}$ ,  $j = 0, 1, \dots, N_1 - 1$ ,  $M_1 = N_1 = 50$ . Moreover, denote

$$Error = \sqrt{\frac{\sum_{i=1}^N (g(x_i, y_i) - f(x_i, y_i))^2}{N}}$$

as the fitting error of the given scattered points  $\{(x_i, y_i)\}_{i=1}^N \subseteq \Omega$ . To demonstrate the accuracy of the proposed algorithm, we perform experiments with four functions: a discontinuous function  $f_1$ , a non-smooth function  $f_2$ , a smooth function  $f_3$  and the Franke test function  $f_4$  as follows.

$$f_1(x, y) = \begin{cases} \frac{x^2 y}{x^2 + y^2}, & x^2 + y^2 \leq 1, \\ x + y, & x^2 + y^2 > 1. \end{cases}$$

$$f_2(x, y) = \begin{cases} \frac{xy}{\sqrt{x^2 + y^2}}, & x^2 + y^2 \leq 1, \\ xy, & x^2 + y^2 > 1. \end{cases}$$

$$f_3(x, y) = \frac{1.25 + \cos(5.4y)}{6 + 6(3x - 1)^2}.$$

$$\begin{aligned} f_4(x, y) &= 0.75 \exp\left[-\frac{(9x-2)^2 + (9y-2)^2}{4}\right] + 0.75 \exp\left[-\frac{(9x+1)^2}{49} - \frac{(9y+1)^2}{10}\right] \\ &+ 0.5 \exp\left[-\frac{(9x-7)^2 + (9y-3)^2}{4}\right] - 0.2 \exp[-(9x-4)^2 - (9y-7)^2]. \end{aligned}$$



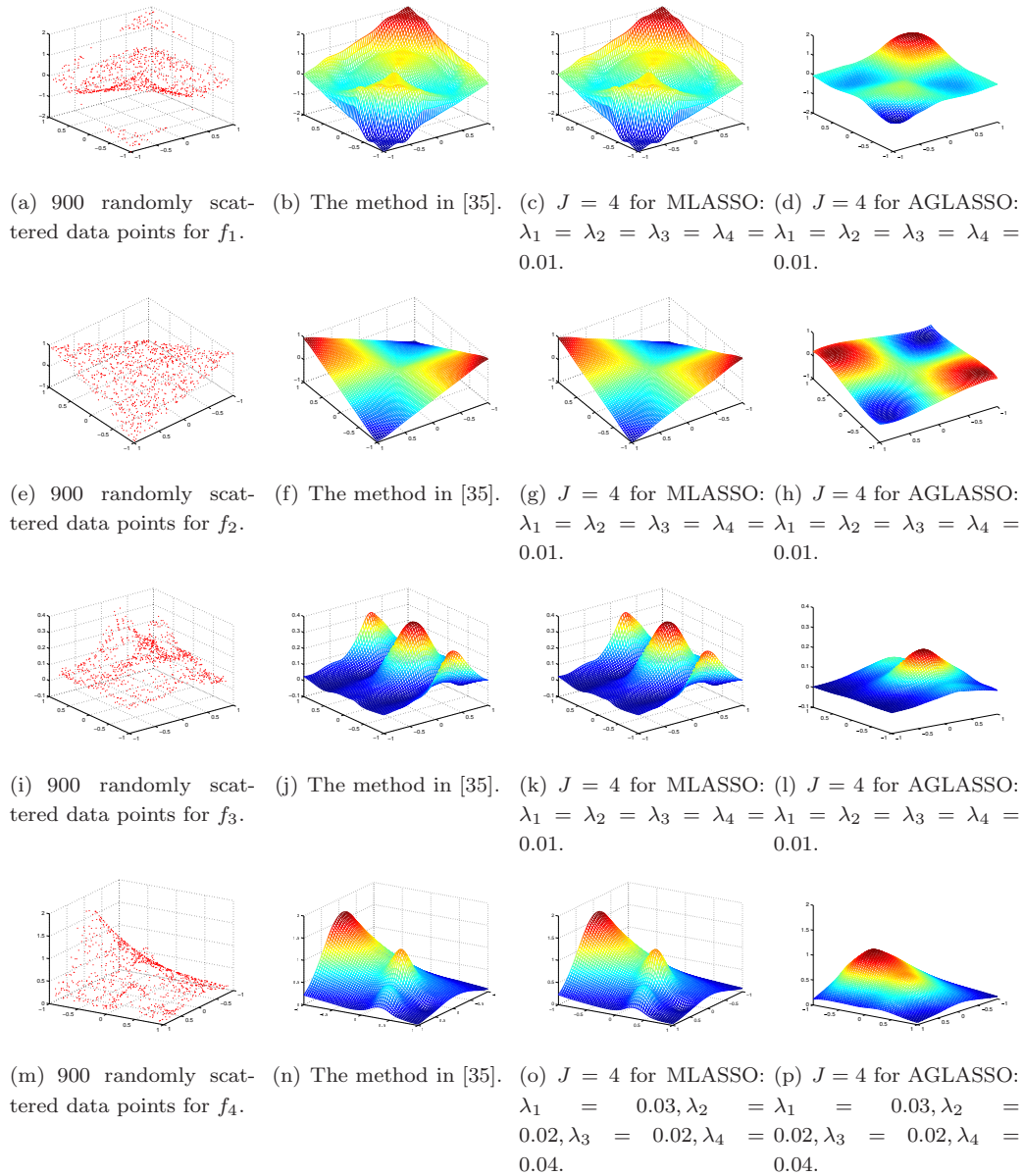
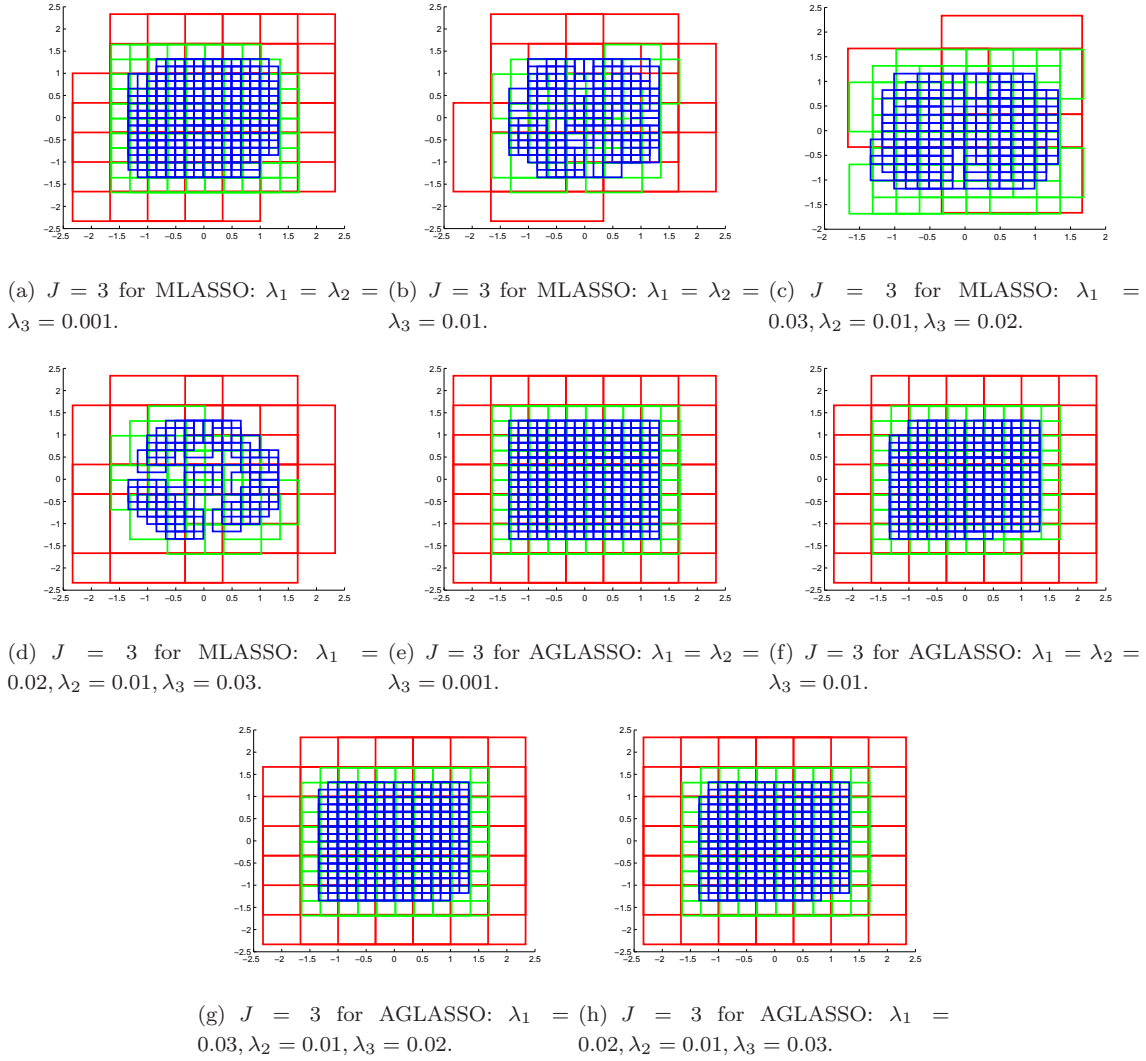
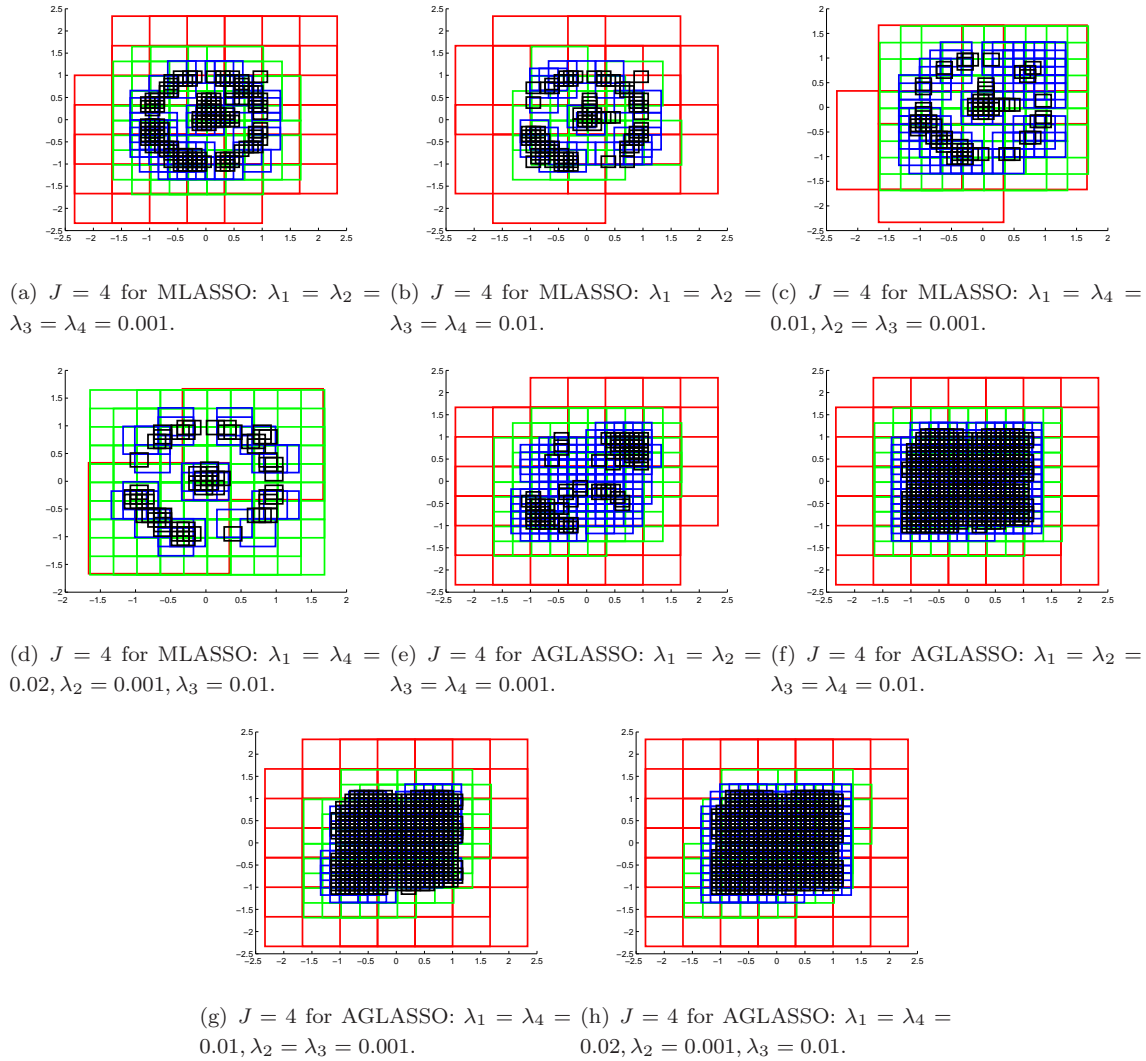


Fig. 1. The scattered data points and the corresponding approximation surfaces: (a)-(d) for  $f_1$ , (e)-(h) for  $f_2$ , (i)-(l) for  $f_3$ , (m)-(p) for  $f_4$ .

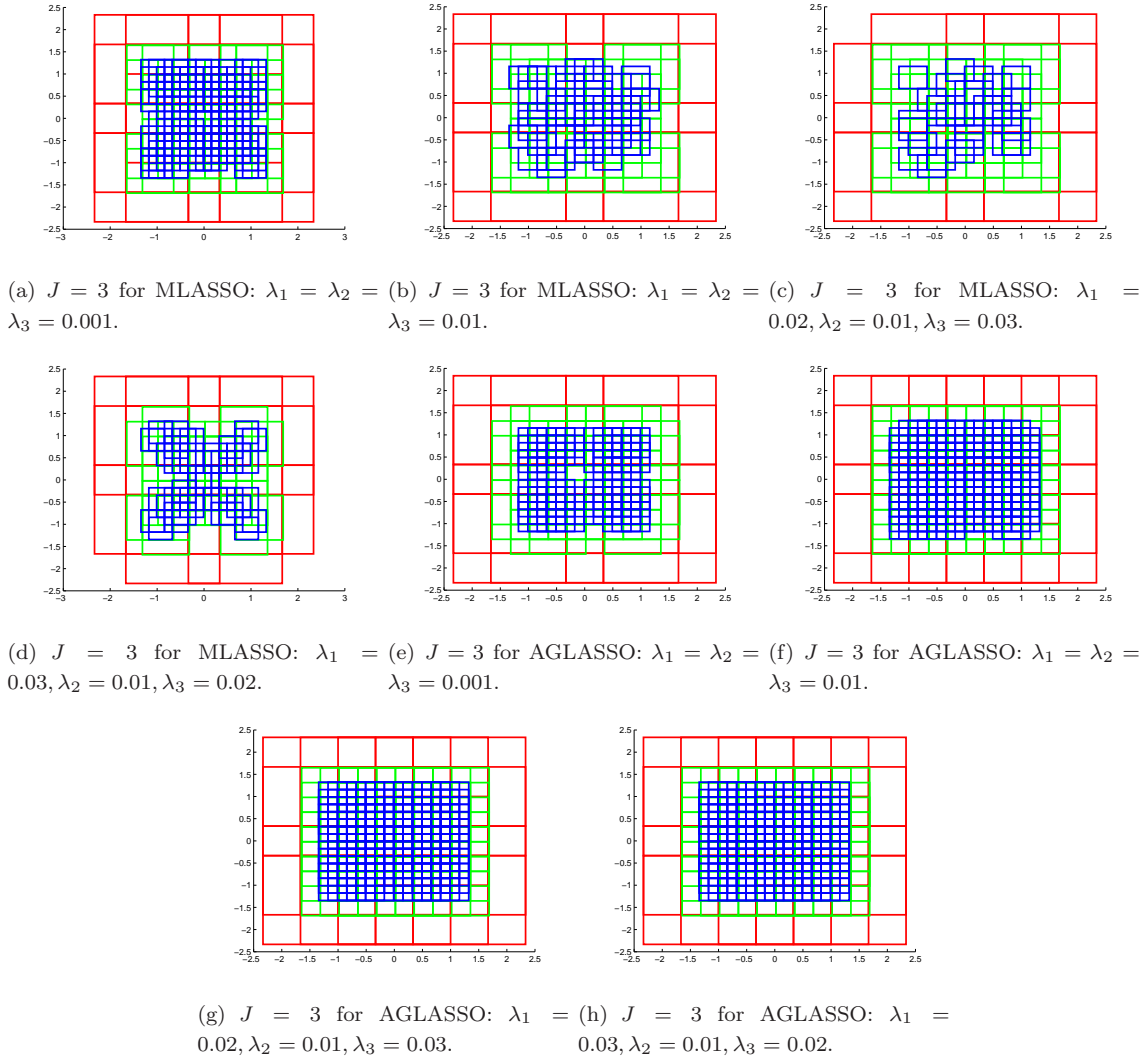


Fig. 2 The distribution of the support for  $f_1$  with  $J = 3$ .Table 1. The  $l_0$  norm and the approximation errors for different parameters shown in Fig.2 for  $f_1$  with  $J = 3$ .

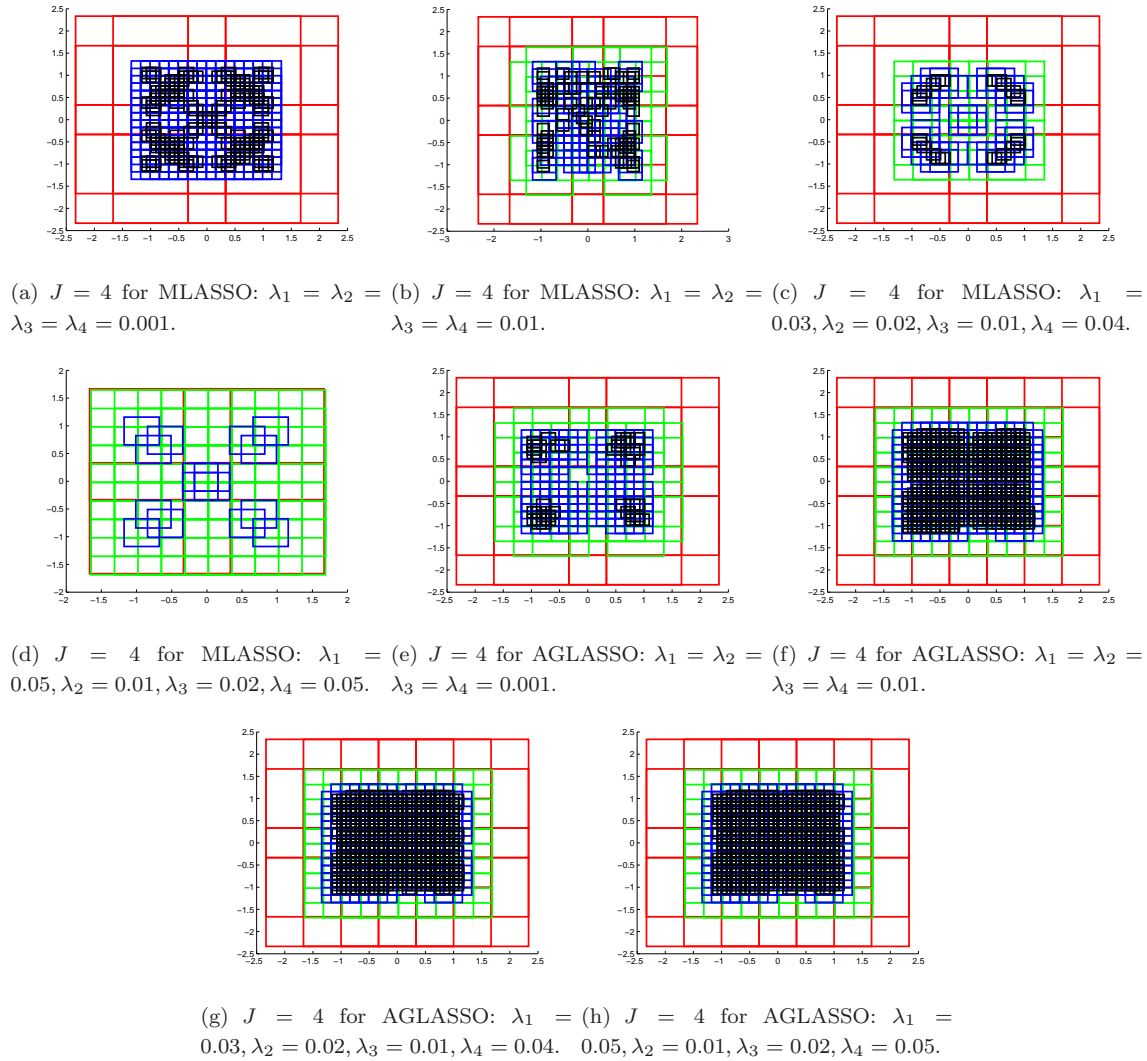
	$(l_0(\mathbf{X}_1), l_0(\mathbf{X}_2), l_0(\mathbf{X}_3))$	Error	RMS	Iterations	Time(sec)
[35]	(24, 64, 193)	2.1241e-3	2.3512e-3	3	0.0241
Fig.2(a)	(18, 53, 143)	2.2538e-3	4.3462e-3	17	0.0431
Fig.2(b)	(13, 29, 84)	3.8215e-3	5.6138e-3	1322	2.0032
Fig.2(c)	(4, 41, 88)	5.1433e-3	7.3768e-3	1841	2.4456
Fig.2(d)	(15, 22, 49)	5.3102e-3	8.7471e-3	2436	3.2345
Fig.2(e)	(20, 51, 116)	5.9973e-1	6.2737e-1	1	0.3917
Fig.2(f)	(24, 61, 181)	5.0691e-1	5.4132e-1	1	0.2961
Fig.2(g)	(24, 63, 190)	4.2005e-1	4.6263e-1	1	0.3524
Fig.2(h)	(25, 62, 189)	3.9211e-1	4.3247e-1	1	0.3012

Fig. 3 The distribution of the support for  $f_1$  with  $J = 4$ .Table 2. The  $l_0$  norm and the approximation errors for different parameters shown in Fig.3 for  $f_1$  with  $J = 4$ .

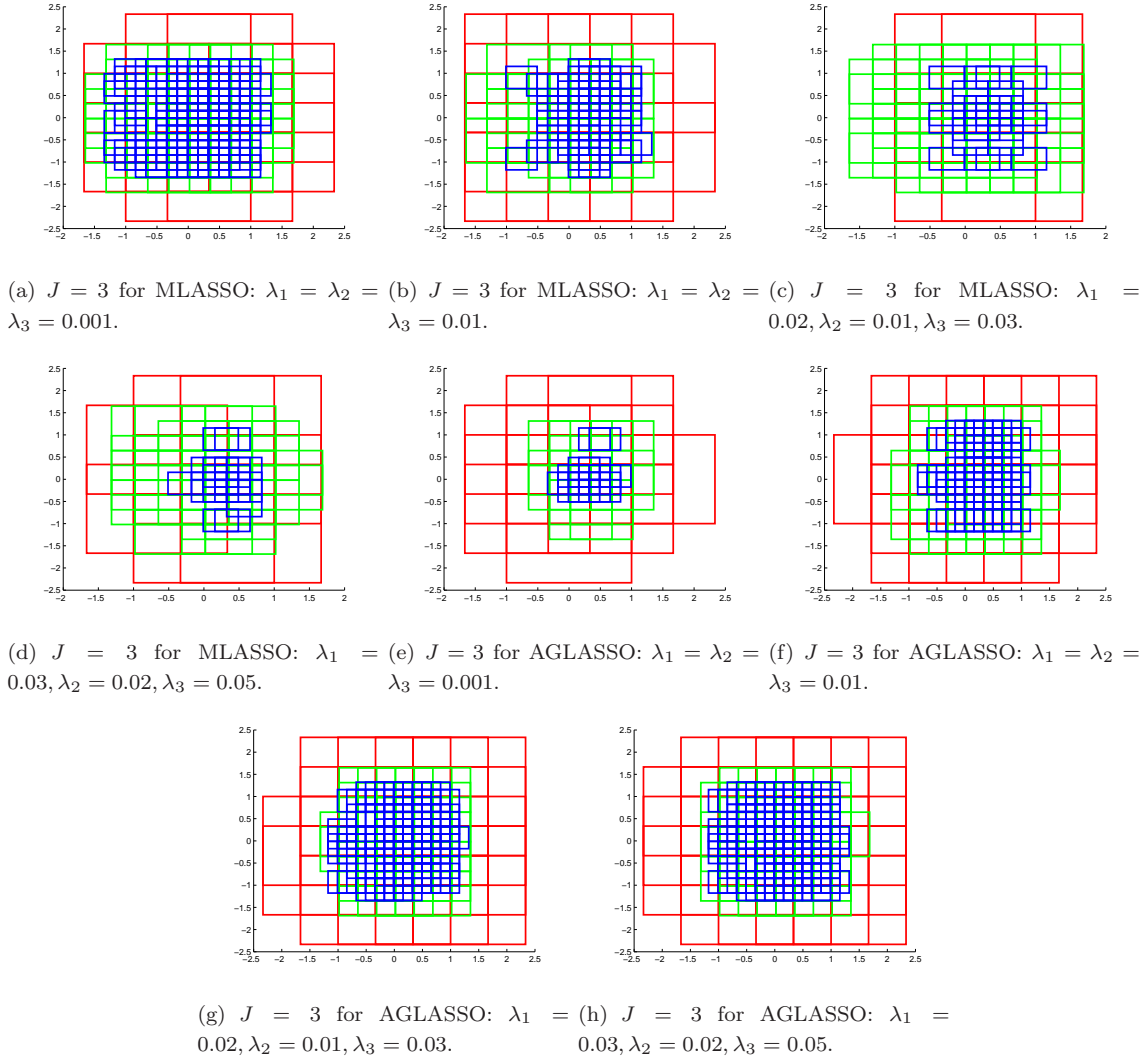
	$(l_0(\mathbf{X}_1), l_0(\mathbf{X}_2), l_0(\mathbf{X}_3), l_0(\mathbf{X}_4))$	Error	RMS	Iterations	Time(sec)
[35]	(25, 62, 192, 674)	1.1185e-3	3.3243e-4	4	0.2191
Fig.3(a)	(17, 37, 50, 138)	1.4298e-3	3.5873e-3	267	4.3145
Fig.3(b)	(15, 21, 27, 88)	2.1073e-3	4.2481e-3	1209	11.1452
Fig.3(c)	(7, 41, 69, 63)	3.1132e-3	5.6871e-3	1307	13.0139
Fig.3(d)	(2, 53, 27, 59)	3.9413e-3	6.1678e-3	1183	12.7346
Fig.3(e)	(20, 52, 114, 90)	5.2471e-1	6.0124e-1	1	5.1328
Fig.3(f)	(23, 61, 181, 537)	5.0109e-1	4.7453e-1	1	5.0129
Fig.3(g)	(24, 48, 112, 544)	5.1902e-1	5.4287e-1	1	4.9879
Fig.3(h)	(25, 45, 176, 581)	3.8716e-1	5.2634e-1	1	4.3472

Fig. 4 The distribution of the support for  $f_2$  with  $J = 3$ .Table 3. The  $l_0$  norm and the approximation errors for different parameters shown in Fig.4 for  $f_2$  with  $J = 3$ .

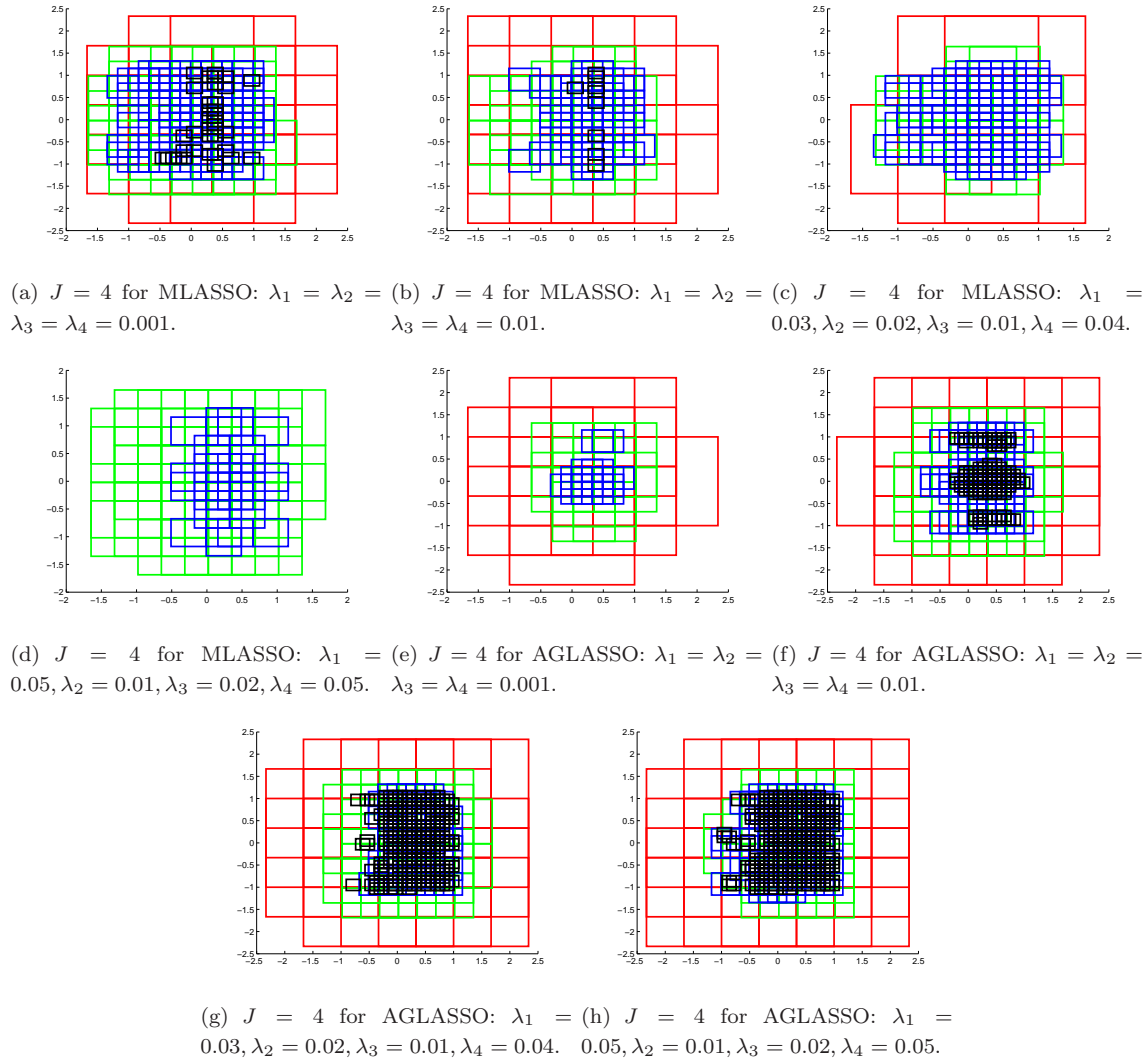
	$(l_0(\mathbf{X}_1), l_0(\mathbf{X}_2), l_0(\mathbf{X}_3))$	Error	RMS	Iterations	Time(sec)
[35]	(22, 64, 194)	3.7541e-3	7.3274e-3	3	0.1102
Fig.4(a)	(18, 41, 115)	4.1637e-3	8.3761e-3	232	0.4257
Fig.4(b)	(16, 41, 53)	5.0749e-3	9.0652e-3	678	2.3091
Fig.4(c)	(15, 40, 31)	4.7049e-3	9.3981e-3	1103	1.6027
Fig.4(d)	(14, 33, 49)	5.2564e-3	9.2971e-3	1089	1.5453
Fig.4(e)	(15, 51, 91)	3.3797e-1	3.5205e-1	1	1.0274
Fig.4(f)	(20, 62, 183)	2.2143e-1	2.6308e-1	1	0.7348
Fig.4(g)	(21, 64, 194)	2.0213e-1	2.1453e-1	1	0.5762
Fig.4(h)	(21, 64, 195)	1.0254e-1	1.2190e-1	1	0.4209

Fig. 5 The distribution of the support for  $f_2$  with  $J = 4$ .Table 4. The  $l_0$  norm and the approximation errors for different parameters shown in Fig.5 for  $f_2$  with  $J = 4$ .

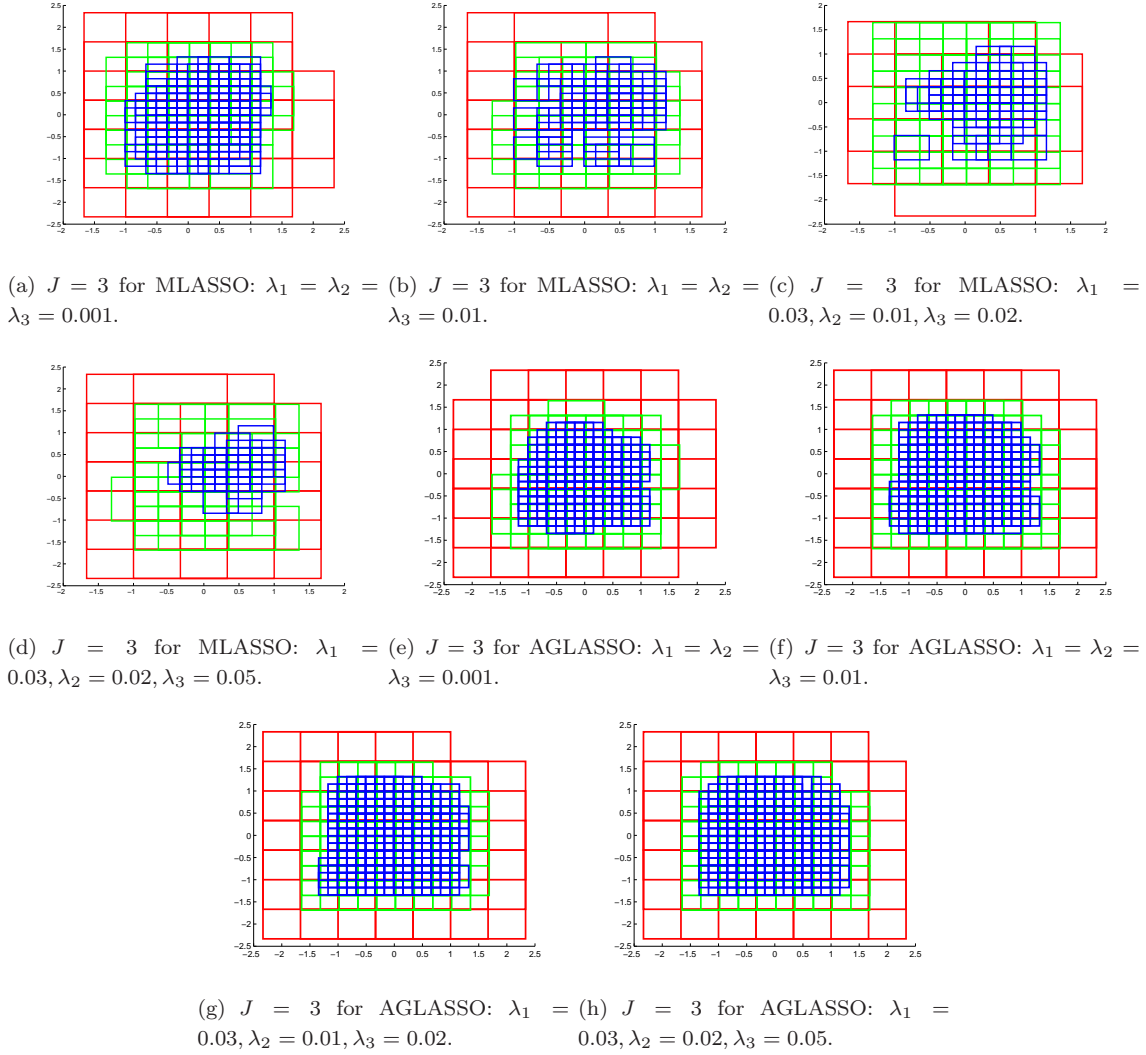
	$(l_0(\mathbf{X}_1), l_0(\mathbf{X}_2), l_0(\mathbf{X}_3), l_0(\mathbf{X}_4))$	Error	RMS	Iterations	Time(sec)
[35]	(22, 63, 195, 673)	2.1342e-3	3.2496e-3	4	0.7326
Fig.5(a)	(16, 28, 45, 73)	3.0054e-3	3.4124e-3	378	5.0312
Fig.5(b)	(17, 31, 77, 54)	2.3321e-3	3.0061e-3	1214	9.7821
Fig.5(c)	(15, 25, 56, 24)	4.1072e-3	5.1132e-3	2601	13.8871
Fig.5(d)	(4, 61, 18, 0)	5.7461e-3	6.3242e-3	3261	15.3487
Fig.5(e)	(16, 52, 91, 40)	1.5002e-1	2.1392e-1	1	5.1902
Fig.5(f)	(20, 64, 185, 471)	1.2301e-1	2.0342e-1	1	4.8106
Fig.5(g)	(21, 64, 180, 589)	2.0039e-1	2.1759e-1	1	4.7951
Fig.5(h)	(20, 64, 185, 596)	3.1402e-1	3.1132e-1	1	4.6283

Fig. 6 The distribution of the support for  $f_3$  with  $J = 3$ .Table 5. The  $l_0$  norm and the approximation errors for different parameters shown in Fig.6 for  $f_3$  with  $J = 3$ .

	$(l_0(\mathbf{X}_1), l_0(\mathbf{X}_2), l_0(\mathbf{X}_3))$	Error	RMS	Iterations	Time(sec)
[35]	(24, 63, 193)	3.0285e-3	5.8147e-3	3	0.0617
Fig.6(a)	(15, 50, 116)	3.0273e-3	6.3044e-3	298	0.5042
Fig.6(b)	(13, 33, 60)	4.1409e-3	7.6258e-3	739	1.0354
Fig.6(c)	(6, 50, 31)	4.8321e-3	7.6578e-3	978	1.3277
Fig.6(d)	(7, 34, 20)	5.1157e-3	9.2785e-3	683	1.0317
Fig.6(e)	(13, 19, 18)	4.6342e-2	5.1462e-2	1	0.5745
Fig.6(f)	(21, 39, 74)	5.7749e-2	6.0324e-2	1	0.4182
Fig.6(g)	(22, 42, 123)	6.7765e-2	7.0079e-2	1	0.6242
Fig.6(h)	(24, 45, 138)	1.1091e-1	1.0072e-1	1	0.1562

Fig. 7 The distribution of the support for  $f_3$  with  $J = 4$ .Table 6. The  $l_0$  norm and the approximation errors for different parameters shown in Fig.7 for  $f_3$  with  $J = 4$ .

	$(l_0(\mathbf{X}_1), l_0(\mathbf{X}_2), l_0(\mathbf{X}_3), l_0(\mathbf{X}_4))$	Error	RMS	Iterations	Time(sec)
[35]	(25, 63, 192, 674)	1.6373e-3	3.8077e-3	4	0.7348
Fig.7(a)	(16, 47, 105, 38)	1.7665e-3	5.6282e-3	573	8.3451
Fig.7(b)	(13, 31, 58, 10)	2.3442e-3	5.6422e-3	978	13.6259
Fig.7(c)	(7, 25, 96, 0)	3.6609e-3	6.4672e-3	854	11.7498
Fig.7(d)	(0, 51, 36, 0)	4.3713e-3	8.7693e-3	1588	19.8770
Fig.7(e)	(14, 18, 19, 0)	4.6868e-2	5.3092e-2	1	5.2829
Fig.7(f)	(20, 38, 73, 119)	5.1103e-2	5.5647e-2	1	5.1456
Fig.7(g)	(22, 46, 68, 279)	6.9144e-2	7.0093e-2	1	4.3378
Fig.7(h)	(23, 34, 101, 328)	1.0138e-1	1.1552e-1	1	3.6595

Fig. 8 The distribution of the support for  $f_4$  with  $J = 3$ .Table 7. The  $l_0$  norm and the approximation errors for different parameters shown in Fig.8 for  $f_4$  with  $J = 3$ .

	$(l_0(\mathbf{X}_1), l_0(\mathbf{X}_2), l_0(\mathbf{X}_3))$	Error	RMS	Iterations	Time(sec)
[35]	(25, 62, 193)	3.2254e-3	5.0711e-3	3	0.0834
Fig.8(a)	(17, 41, 110)	3.7421e-3	6.3902e-3	19	1.1642
Fig.8(b)	(15, 34, 57)	4.0324e-3	6.2097e-3	938	1.7439
Fig.8(c)	(9, 38, 46)	4.5021e-3	8.1093e-3	1463	2.4762
Fig.8(d)	(15, 29, 33)	6.2043e-3	8.0072e-3	2230	2.7803
Fig.8(e)	(21, 45, 126)	2.0414e-1	6.0056e-1	1	0.7439
Fig.8(f)	(24, 60, 161)	2.1369e-1	3.1057e-1	1	0.5648
Fig.8(g)	(23, 57, 166)	3.2451e-1	2.2731e-1	1	0.4846
Fig.8(h)	(24, 58, 179)	5.3021e-1	2.1237e-1	1	0.4218



Table 8. The  $l_0$  norm and the approximation errors for different parameters shown in Fig.9 for  $f_4$  with  $J = 4$ .

	$(l_0(\mathbf{X}_1), l_0(\mathbf{X}_2), l_0(\mathbf{X}_3), l_0(\mathbf{X}_4))$	Error	RMS	Iterations	Time(sec)
[35]	(25, 63, 194, 675)	4.1124e-4	3.2017e-3	4	2.1406
Fig.9(a)	(14, 34, 84, 108)	5.0121e-4	5.0512e-3	687	12.1132
Fig.9(b)	(15, 33, 48, 31)	1.18974e-3	4.6645e-3	1152	18.4120
Fig.9(c)	(13, 27, 52, 8)	4.1321e-3	7.1452e-3	1333	18.2461
Fig.9(d)	(12, 22, 70, 6)	4.2134e-3	7.6731e-3	2231	28.1121
Fig.9(e)	(22, 47, 126, 145)	1.5782e-1	1.7287e-1	1	5.1631
Fig.9(f)	(24, 58, 163, 491)	2.2056e-1	2.2142e-1	1	5.4315
Fig.9(g)	(24, 58, 164, 557)	3.0349e-1	3.4397e-1	1	4.3341
Fig.9(h)	(25, 60, 160, 524)	5.2570e-1	5.3329e-1	1	3.9764

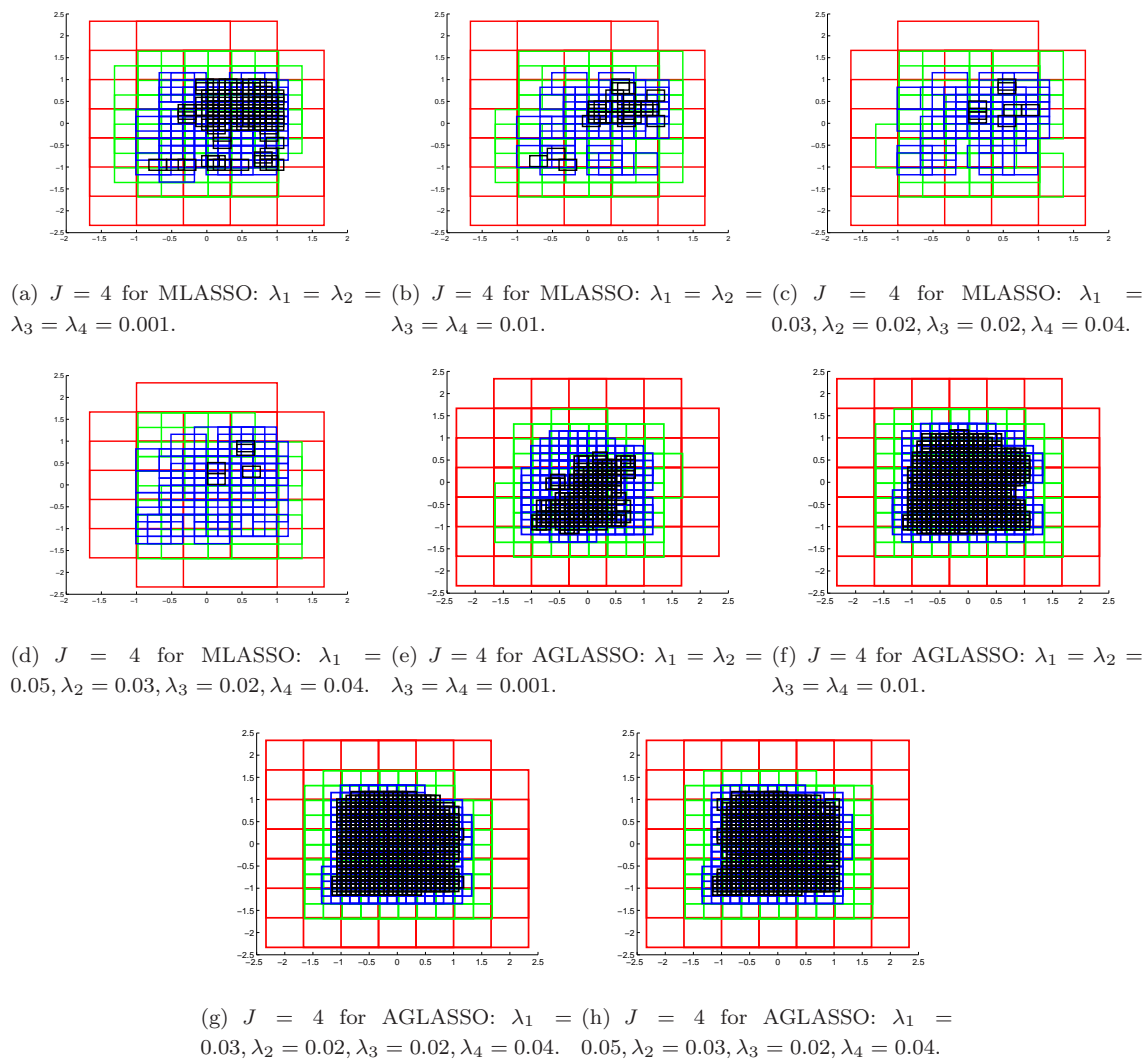


Fig. 9 The distribution of the support for  $f_4$  with  $J = 4$ .

For the numerical implementation in this paper, we employ the 2D tensor product quadratic B-spline as the function  $\varphi$ . We show that such a simple system with the Algorithm 1 can be used to effectively reconstruct surface of sparse representation from a scattered data set. The choices of the threshold  $\sigma, \epsilon$  can be chosen according to the accuracy and sparsity. We consider the four functions with  $\sigma = 10^{-3}, \epsilon = 10^{-4}, N = 900$  and the 900 scattered points are chosen randomly. Moreover, we compare Algorithm 1 with the basic MBA algorithm presented in [35] under the termination condition  $|\Delta g_j| \leq O(10^{-3})$  and the AGLASSO model, both applying the same thresholding  $\sigma = 10^{-3}$  as Algorithm 1 to their results.

We experiment the above three methods for  $J = 3$  and  $J = 4$  starting from level 1 with  $5 \times 5$  biquadratic B-spline functions respectively. Fig.1 shows the scattered data points and the corresponding approximations of the four functions with Algorithm 1, the method in [35] and the AGLASSO model respectively. Fig.2-9 illustrate the distribution of the support of the B-spline functions with nonzero coefficients for  $J = 3$  and  $J = 4$  respectively. The red, green, blue and black rectangles denote the support of the B-splines corresponding to  $\mathbf{X}_1, \mathbf{X}_2, \mathbf{X}_3$  and  $\mathbf{X}_4$  respectively. Moreover, Tables 1-8 give the approximation accuracy, the iterations, the running time and the  $l_0$  norm of the solution with different parameters for  $f_1 - f_4$ , where the length of  $\mathbf{X}_1, \mathbf{X}_2, \mathbf{X}_3$  and  $\mathbf{X}_4$  is 25, 64, 196 and 625 respectively. In addition, all our calculations are done in Matlab on a laptop with Inter Core i7 (2.90GHZ) CPU and 8.0G RAM.

**Discussion 1.** The numerical results demonstrate that Algorithm 1 and the method in [35] have almost the same approximation errors, while Algorithm 1 obtains the sparse solution. Compared with the AGLASSO model, Algorithm 1 provides the sparser solutions with less error, though more iterations and more time.

Through the first two steps of Algorithm 1, we can obtain an approximation solution of the MLASSO model with no sparsity and the solution has some big components and some small ones which reflect different importance and contribution. Then by step three, we throw out small components of the computed solution which means we keep only the important ones with great contribution to the solution. Therefore, by choosing appropriate regularization parameters, the final solution can indicate the important parts we are interested in and identify the important features within the selected levels simultaneously of the exact surface since they are all determined by the big components. Experiment results verify this conclusion.

Taken together, Algorithm 1 can reconstruct the test functions reasonably with a sparse representation within a few levels by choosing some appropriate regularization parameters.

## 4 Conclusion

This paper presents an approach for scattered data fitting using the PSI space and the  $l_1$  regularization. It is concluded into the MLASSO model which allows us to balance the accuracy and the sparsity of the fitting surface. The model can be solved using Algorithm 1 with the ADMM algorithm. Numerical examples demonstrate that compared to the basic MBA algorithm in [35] and the AGLASSO model, the MLASSO model provides an efficient, sparse, flexible and reasonable solution. Moreover, the distribution of the basis functions of the sparse solution can identify the regions of the underlying surface where large fluctuations occur.

**Acknowledgements** This work was supported by the National Natural Science Foundation of China (Nos.11526098, 11001037, 11290143, 11471066), the Research Foundation for Advanced Talents of Jiangsu University (No.14JDG034), the Natural Science Foundation of Jiangsu Province (No.BK20160487) and the Fundamental Research Funds for the Central Universities (DUT15LK44).

## References

- 1 F. Bauer, O. Ivanysyn. Optimal regularization with two interdependent regularization parameters. *Inverse Probl.*, 2007, 23: 331–342

- 2 F. Bauer, S. V. Pereverzev. An utilization of a rough approximation of a noise covariance within the framework of multi-parameter regularization. *Int. J. Tomogr. Stat.*, 2006, 4: 1–12
- 3 M. Belge, M. E. Kilmer, E. L. Miller. Efficient determination of multiple regularization parameters in a generalized L-curve framework, *Inverse Probl.*, 2002, 18: 1161–1183
- 4 M. Benzi. Preconditioning Techniques for Large Linear Systems: A Survey. *J. Comput. Phys.*, 2002, 182: 418–477
- 5 S. Boyd, N. Parikh, E. Chu, B. Peleato, J. Eckstein. Distributed optimization and statistical learning via the alternating direction method of multipliers. *Foundations and Trends of Machine Learning*, 2010, 3: 1–122
- 6 C. Brezinski, M. Redivo-Zaglia, G. Rodriguez, S. Seatzu. Multi-parameter regularization techniques for ill-conditioned linear systems. *Numer. Math.*, 2003, 94: 203–228
- 7 E. J. Candès, J. Romberg, T. Tao. Robust uncertainty principles: Exact signal reconstruction from highly incomplete frequency information. *IEEE Trans. Inform. Theory*, 2006, 52(2): 489–509
- 8 E. J. Candès, J. Romberg, T. Tao. Stable signal recovery from incomplete and inaccurate measurements. *Comm. Pure Appl. Math.*, 2006, 59(8): 1207–1223
- 9 E. J. Candès, T. Tao. Decoding by linear programming. *IEEE Trans. Inform. Theory*, 2005, 51(12): 4203–4215
- 10 E. J. Candès, T. Tao. Near-optimal signal recovery from random projections: Universal encoding strategies. *IEEE Trans. Inform. Theory*, 2006, 52(12): 5406–5425
- 11 D. Castaño, A. Kunoth. Adaptive fitting of scattered data by spline-wavelets. In: *Curves and Surfaces*, Vanderbilt University Press, 2003
- 12 Z. Chen, Y. Lu, Y. Xu, H. Yang. Multi-parameter Tikhonov regularization for linear ill-posed operator equations. *J. Comp. Math.*, 2008, 26: 37–55
- 13 A. Cohen, W. Dahmen, R. DeVore. Compressed sensing and best k-term approximation. *J. Amer. Math. Soc.*, 2009, 22: 211–231
- 14 C. de Boor, A. Ron. Fourier analysis of the approximation power of principal shift-invariant spaces. *Constr. Approx.*, 1992, 8(4): 427–462
- 15 R. A. DeVore, B. Jawerth, B. J. Lucier. Surface compression. *Comput. Aided Geom. Des.*, 1992, 9: 219–239
- 16 B. Dong, Z. Shen. Wavelet frame based surface reconstruction from unorganized points. *J. Comput. Phys*, 2011, 230: 8247–8255
- 17 D. Donoho. De-noising by soft-thresholding. *IEEE Trans. Inform. Theory*, 1995, 41(3): 613–627
- 18 J. Douglas, H. H. Rachford. On the numerical solution of heat conduction problems in two and three space variables. *Trans. Amer. Math. Soc.*, 1956, 82: 421–439
- 19 J. Eckstein. Splitting methods for monotone operators with applications to parallel optimization. Ph.D. thesis, Massachusetts Institute of Technology, 1989, 16(6): 964–979
- 20 J. Eckstein, D. Bertsekas. On the Douglas-Rachford splitting method and the proximal point algorithm for maximal monotone operators. *Mathematical Programming* 55, North Holland, 1992
- 21 E. Esser. Applications of Lagrangian-based alternating direction methods and connections to split Bregman. *CAM Report 09-31*, UCLA, 2009
- 22 M. Fasi, J. Langou, Y. Robert, B. Ucare. A backward/forward recovery approach for the preconditioned conjugate gradient method. *J. Comput. Sci.*, 2016, 17: 522–534
- 23 D. R. Forsey, R. H. Bartels. Surface fitting with hierarchical splines. *ACM Trans. on Graphics*, 1995, 14(2): 134–161
- 24 D. Gabay, B. Mercier. A dual algorithm for the solution of nonlinear variational problems via finite element approximations. *Comp. Math. Appl*, 1976, 2: 17–40
- 25 I. Gijbels, A. Lambert, P. Qiu. Edge-preserving image denoising and estimation of discontinuous surfaces. *IEEE Trans. Pattern Anal. Machine Intell*, 2006, 28(7): 1075–1087
- 26 T. Goldstein, S. Osher. The split Bregman method for  $l_1$ -regularized problems. *SIAM J. Imaging Sci*, 2009, 2(2): 323–343
- 27 M. Hanke, O. Scherzer. Inverse problems light: numerical differentiation. *Amer. Math. Monthly*, 2001, 108(6): 512–521
- 28 D. N. Hào, L. H. Chuong, D. Lesnic. Heuristic regularization methods for numerical differentiation. *Comput. Math. Appl*, 2012, 63: 816–826
- 29 B. He, X. Yuan. On the  $O(\frac{1}{n})$  convergence rate of Douglas-Rachford alternating direction method. *SIAM J. Numer. Anal.*, 2012, 50: 700–709
- 30 H. Ji, Z. Shen, Y. H. Xu. Wavelet frame based scene reconstruction from range data. *J. Comput. Phys*, 2010, 229(6): 2093–2108
- 31 R. Q. Jia. The Toeplitz theorem and its applications to approximation theory and linear PDEs. *Trans. Amer. Math. Soc*, 1995, 347(7): 2585–2594
- 32 M. J. Johnson, Z. Shen, Y. H. Xu. Scattered data reconstruction by regularization in B-spline and associated wavelet spaces. *J. Approx. Theory* 2009, 159: 197–223
- 33 S. Kunis, H. Rauhut. Random sampling of sparse trigonometric polynomials II-orthogonal matching pursuit versus basis pursuit. *Found. Comput. Math.* 2008, 8(6): 737–763

- 34 B. G. Lee, J. J. Lee, K. R. Kwon. Quasi-interpolants based multilevel B-spline surface reconstruction from scattered data. *International Conference on Computational Science and Its Applications*, 2005, 1209–1218
- 35 S. Y. Lee, G. Wolberg, S. Y. Shin. Scattered data interpolation with multilevel B-splines. *IEEE Trans. Visualization Comput. Graph*, 1997, 3(3): 229–244
- 36 P. L. Lions, B. Mercier. Splitting algorithms for the sum of two nonlinear operators. *SIAM J. Numer. Anal.*, 1979, 16(6): 964–979
- 37 S. Lu, S. V. Pereverzer. Multi-parameter regularization and its numerical realization. *Numer. Math.*, 2011, 118: 1–31
- 38 M. R. M. Bozzini. Testing methods for 3D scattered data interpolation. *Monografías de la Académica de Ciencias de Zaragoza*, 2002, 20: 111–135
- 39 L. Meier, S. van de Geer, P. Bühlmann. The group lasso for logistic regression. *J. Roy. Statist. Soc. Ser. B*, 2008, 70: 53–71
- 40 D. Phillips. A technique for the numerical solution of certain integral equation of the first kind. *J. Assoc. Comput. Mach.*, 1962, 9: 84–97
- 41 H. Rauhut. Random sampling of sparse trigonometric polynomials. *Appl. Comput. Harmon. Anal.*, 2007, 22(1): 16–42
- 42 H. Rauhut. Stability results for random sampling of sparse trigonometric polynomials. *IEEE Trans. Inform. Theory*, 2008, 54(12): 5661–5670
- 43 A. M. Sajo-Castelli, M. A. Fortes, M. Raydana. Preconditioned conjugate gradient method for finding minimal energy surfaces on Powell-Sabin triangulations. *J. Comput. App. Math.*, 2014, 268: 34–55
- 44 F. J. M. Schmitt, B. A. Barsky, W. H. Du. An adaptive subdivision method for surface fitting from sampled data. *Comput. Graph.*, 1986, 20(4): 179–188
- 45 S. Setzer. Split bregman algorithm, douglas-rachfordsplitting and frame shrinkage. In: *Proceedings of the Second International Conference on Scale Space Methods and Variational Methods in Computer Vision*, 2009
- 46 G. Steidl, T. Teuber. Removing Multiplicative Noise by Douglas-Rachford Splitting Methods. *J. Math. Imaging. Vis.*, 2010, 36(2): 168–184
- 47 R. Stevenson, B. Schmitz, E. Delp. Discontinuity preserving regularization of inverse visual problems. *IEEE Trans. Systems, Man and Cybernetics*, 1994, 3: 455–469
- 48 R. Tibshirani. Regression shrinkage and selection via the Lasso. *J. Roy. Statist. Soc. Ser. B*, 1996, 58: 267–288
- 49 H. Wang, C. Leng. A note on adaptive group lasso. *Comput. Statist. Data Anal.*, 2008, 52: 5277–5286
- 50 Y. B. Wang, Y. C. Hon, J. Cheng. Reconstruction of high order derivatives from input data. *J. Inverse Ill-Posed Probl.*, 2009, 14(2): 205–218
- 51 Z. Wang, J. Yu, X. Xie. An improved algorithm for surface fitting based on B-spline function. *Information and Computing (2011 Fourth International Conference on)* 80–82
- 52 C. Wu, X-C. Tai. Augmented Lagrangian method, Dual methods and Split-Bregman Iterations for ROF, vectorial TV and higher order models. *SIAM J. Imaging Science*, 2010, 3(3): 300–339
- 53 M. Yuan, Y. Lin. Model selection and estimation in regression with grouped variables. *The Royal Statistical Society*, 2006, 68: 49–76
- 54 X. M. Yuan. Alternating direction method for covariance selection models. *J. Sci. Comput.*, 2012, 51: 261–273
- 55 H. Zou. The adaptive lasso and its oracle properties. *J. Am. Stat. Assoc.*, 2006, 101: 1418–1429